

Estimation of Chilling and Heat Accumulation Periods Based on the Timing of Olive Pollination

Jesús Rojo ¹, Fabio Orlandi ^{2,*}, Ali Ben Dhiab ³, Beatriz Lara ¹, Antonio Picornell ⁴, Jose Oteros ⁵, Monji Msallem ³, Marco Fornaciari ² and Rosa Pérez-Badia ¹

¹ University of Castilla-La Mancha Institute of Environmental Sciences (Botany), Toledo, Spain;
jesus.rojo.ubeda@gmail.com (J.R.); beatriz.lara@uclm.es (B.L.); rosa.perez@uclm.es (R.P.-B.)

² Department of Civil and Environmental Engineering, University of Perugia, Perugia, Italy;
fabio.orlandi@unipg.it (F.O.); marco.fornaciari@unipg.it (M.F.)

³ Laboratory of Palynology, Olive Tree Institute, Tunis, Tunisia; bendhiabali@yahoo.fr (A.B.D.);
msallemonji@yahoo.fr (M.M.)

⁴ Department of Botany and Plant Physiology, University of Malaga, Malaga, Spain; picornell@uma.es
(A.P.)

⁵ Department of Botany, Ecology and Plant Physiology, University of Cordoba, Cordoba, Spain;
oterosjose@gmail.com (J.O.)

* Correspondence: fabio.orlandi@unipg.it

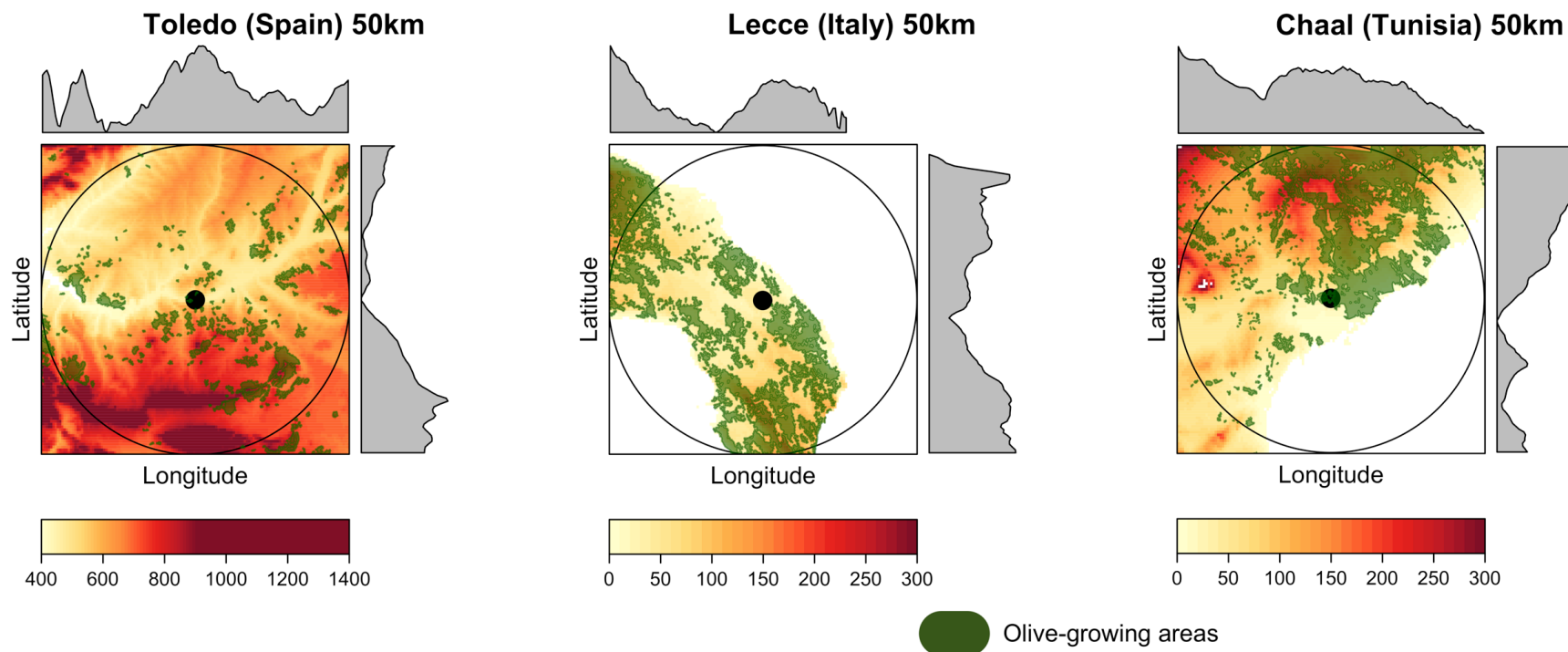


Figure S1. Topographical characterization of the three sampling stations (Toledo, Lecce and Chaal) and olive crops in the surrounding areas (50 km). Digital elevation model provided by the Worldclim project (Fick and Hijmans, 2017), and olive-growing map provided by the CORINE Land project (European Union, Copernicus Land Monitoring Service, 2020).

Table S1. Climatic data for Toledo (Spain). Latitude: 39° 51' N, Longitude: 04° 02' W, Altitude: 450 m ASL

	Mean temperature (°C)	Maximum temperature (°C)	Minimum temperature (°C)	Rainfall
January	6.6	11.3	2.0	30.2
February	8.1	13.3	2.9	29.5
March	10.9	16.9	5.0	32.2
April	13.3	19.3	7.3	40.3
May	17.3	23.7	11.0	38.8
June	22.7	29.7	15.7	22.5
July	26.4	34.0	18.8	7.9
August	26.0	33.5	18.6	8.5
September	21.8	28.6	15.0	21.3
October	16.1	21.8	10.4	44.5
November	10.4	15.3	5.5	40.8
December	7.0	11.4	2.6	39.1
Year	15.6	21.5	9.6	355.7

Bioclimatic diagnosis:

Thermicity index (It): 288

Compensated thermicity index (Itc): 297

Simple continentality index (Ic): 19.8

Diurnality index (Id): 15.2

Annual ombrothermic index (Io): 1.9

Annual positive temperature (Tp): 1867

Annual negative temperature (Tn): 0

Estival temperature (Ts): 751

Positive precipitation (Pp): 356

Latitudinal belt: Eutemperate

Continentality: Oceanic - High Semicontinental

Bioclimate: Mediterranean Xeric - Oceanic

Bioclimate belt: Low Mesomediterranean Upper Semiarid

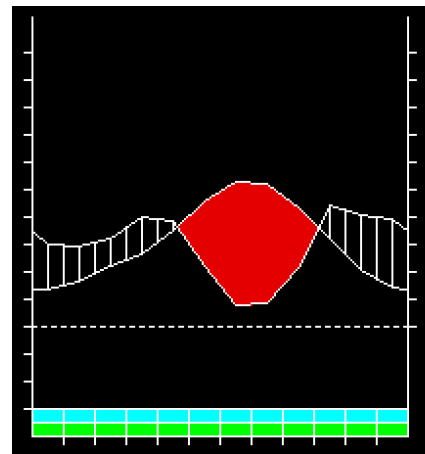


Figure S2. Bioclimatic characterization of Toledo (Spain) according to the bioclimatic classification proposed by Rivas-Martínez et al. (2017) using the bioclimatic diagnosis from WorldWide Bioclimatic Classification System (Rivas-Martínez et al., 2011). Climatic data provided by European Climate Assessment & Dataset (Cornes et al., 2018; Klein Tank et al., 2002) for 50-year period (1969-2018).

Table S2. Climatic data for Lecce (Italy). Latitude: 40° 25' N, Longitude: 18° 03' E, Altitude: 36 m ASL

	Mean temperature (°C)	Maximum temperature (°C)	Minimum temperature (°C)	Rainfall (mm)
January	10.0	12.9	7.1	61.9
February	10.1	13.2	7.1	60.1
March	11.8	15.0	8.6	61.3
April	14.3	17.8	10.9	38.7
May	18.5	22.2	14.8	24.7
June	22.6	26.3	18.8	14.6
July	25.3	29.1	21.5	9.1
August	25.6	29.3	21.9	14.7
September	22.4	26.0	18.9	47.4
October	18.5	21.7	15.3	70.7
November	14.4	17.4	11.4	82.7
December	11.1	14.0	8.2	70.0
Year	17.1	20.4	13.7	556.7

Bioclimatic diagnosis:

Thermicity index (It): 371
 Compensated thermicity index (Itc): 371
 Simple continentality index (Ic): 15.6
 Diurnality index (Id): 7.6
 Annual ombrothermic index (Io): 2.7
 Annual positive temperature (Tp): 2047
 Annual negative temperature (Tn): 0
 Estival temperature (Ts): 735
 Positive precipitation (Pp): 557
 Latitudinal belt: Eutemperate
 Continentality: Oceanic - Low Euoceanic
 Bioclimate: Mediterranean Pluviseasonal - Oceanic
 Bioclimate belt: Upper Thermomediterranean Low Dry

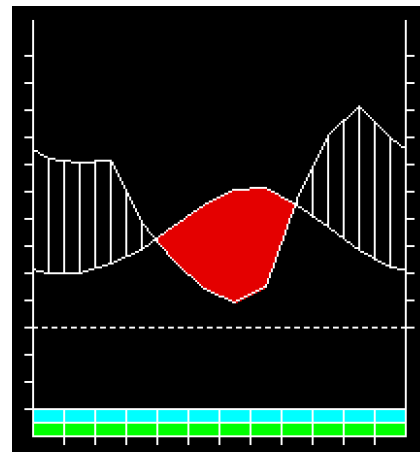


Figure S3. Bioclimatic characterization of Lecce (Italy) according to the bioclimatic classification proposed by Rivas-Martínez et al. (2017) using the bioclimatic diagnosis from WorldWide Bioclimatic Classification System (Rivas-Martínez et al., 2011). Climatic data provided by European Climate Assessment & Dataset (Cornes et al., 2018; Klein Tank et al., 2002) for 50-year period (1969-2018).

Table S3. Climatic data for Chaal (Tunisia). Latitude: 34° 34' N, Longitude: 10° 19' E, Altitude: 78 m ASL.

	Mean temperature (°C)	Maximum temperature (°C)	Minimum temperature (°C)	Rainfall (mm)
January	12.0	16.9	7.1	19.6
February	13.0	18.1	7.9	10.9
March	15.1	20.2	9.9	12.3
April	17.6	22.6	12.6	9.9
May	21.3	26.3	16.3	5.9
June	24.9	30.0	19.9	2.6
July	27.4	32.7	22.0	0.4
August	28.2	33.4	23.0	1.5
September	26.0	30.7	21.3	13.3
October	22.1	26.9	17.3	19.4
November	17.0	21.9	12.0	15.9
December	13.0	17.8	8.3	21.8
Year	19.8	24.8	14.8	133.6

Bioclimatic diagnosis:

Thermicity index (It): 438
 Compensated thermicity index (Itc): 438
 Simple continentality index (Ic): 16.2
 Diurnality index (Id): 10.8
 Annual ombrothermic index (Io): 0.6
 Annual positive temperature (Tp): 2376
 Annual negative temperature (Tn): 0
 Estival temperature (Ts): 805
 Positive precipitation (Pp): 134
 Latitudinal belt: Subtropical
 Continentality: Oceanic - Low Euoceanic
 Bioclimate: Mediterranean Desertic - Oceanic
 Bioclimate belt: Low Thermomediterranean Low Arid

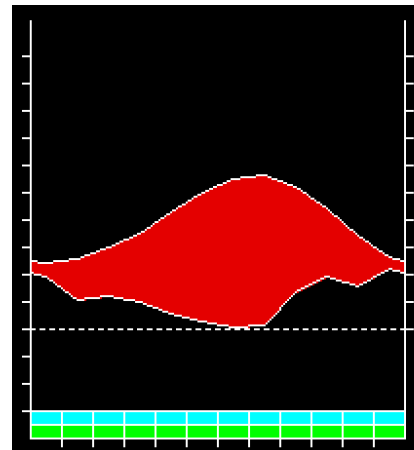


Figure S4. Bioclimatic characterization of Chaal (Tunisia) according to the bioclimatic classification proposed by Rivas-Martínez et al. (2017) using the bioclimatic diagnosis from WorldWide Bioclimatic Classification System (Rivas-Martínez et al., 2011). Climatic data provided by European Climate Assessment & Dataset (Cornes et al., 2018; Klein Tank et al., 2002) for 50-year period (1969-2018).

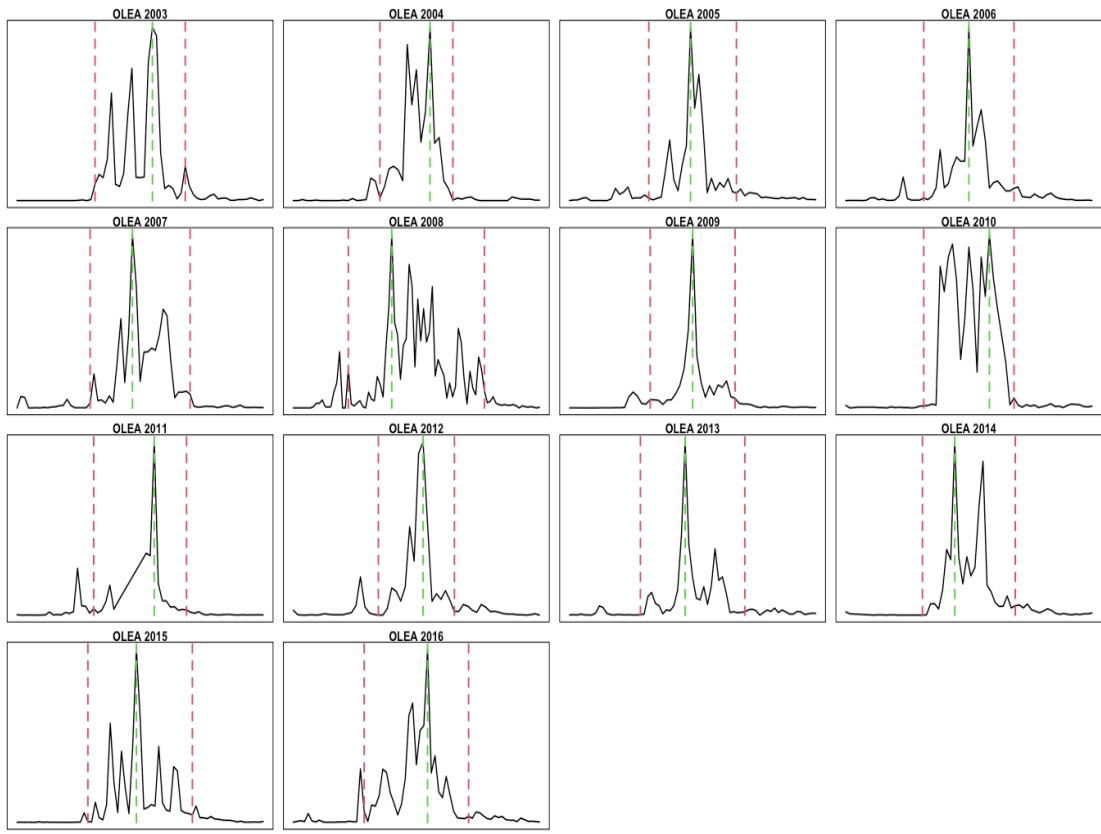


Figure S5. Calculation of the pollen season according to the logistic method for the entire pollen time-series for Toledo (Spain). Red lines represent start and end-dates of the pollen season, respectively, and red line represents peak-date. Graphical output provided by the AeRobiology R package (Rojo et al., 2019). The average percentage of total pollen registered before the start-date of the pollen season in Toledo was 4.8%.

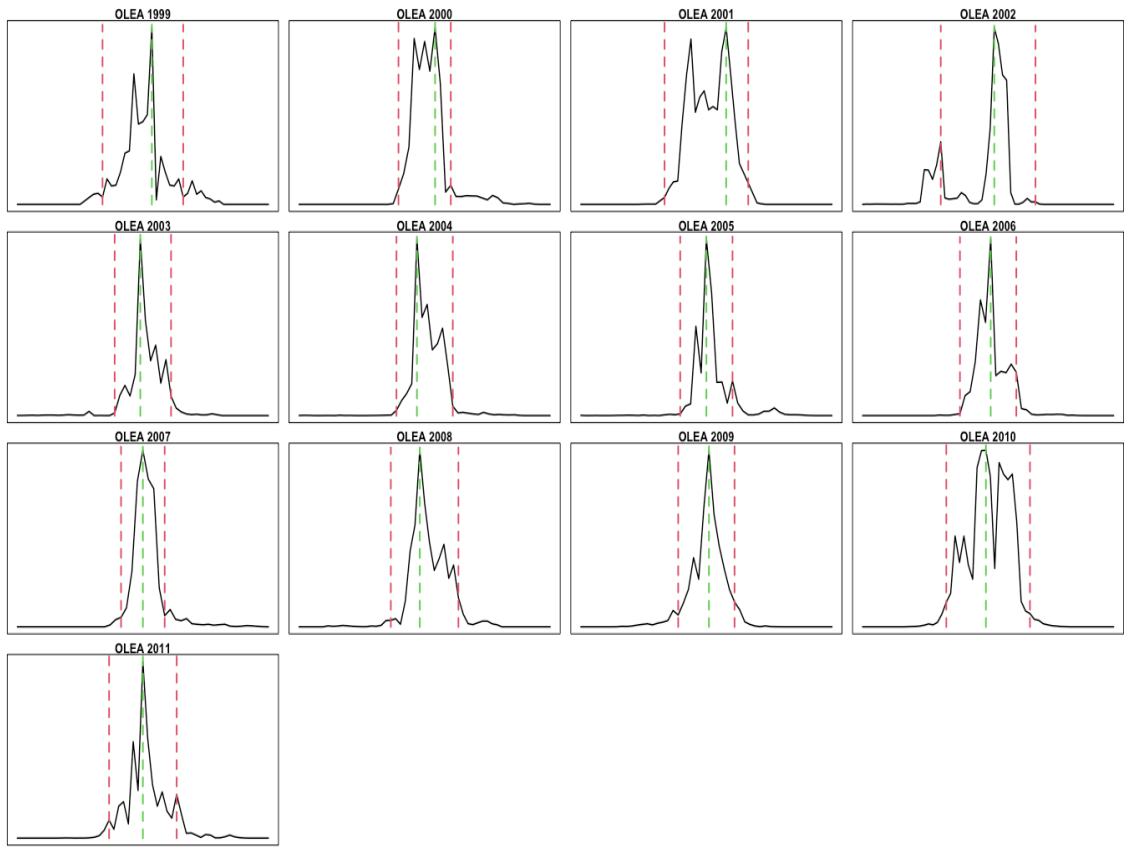


Figure S6. Calculation of the pollen season according to the logistic method for the entire pollen time-series for Lecce (Italy). Red lines represent start and end-dates of the pollen season, respectively, and red line represents peak-date. Graphical output provided by the AeRobiology R package (Rojo et al., 2019). The average percentage of total pollen registered before the start-date of the pollen season in Lecce was 2.4 %.

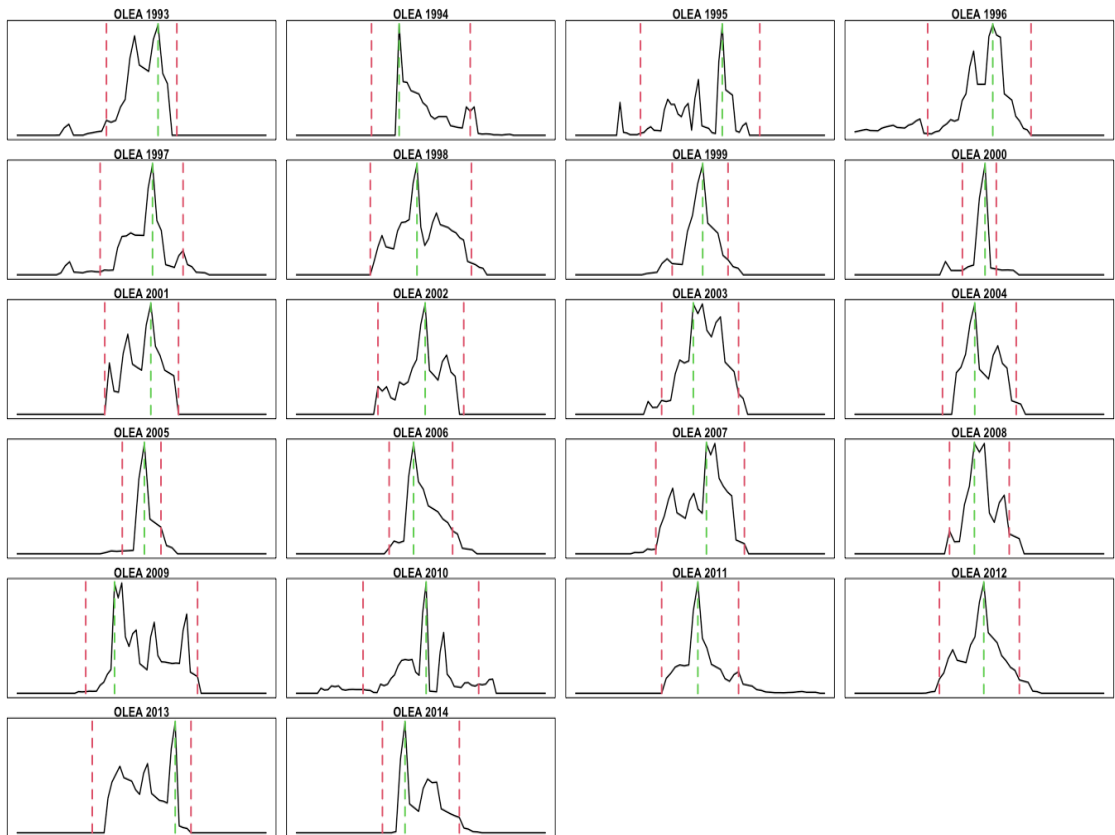


Figure S7. Calculation of the pollen season according to the logistic method for the entire pollen time-series for Chaal (Tunisia). Red lines represent start and end-dates of the pollen season, respectively, and red line represents peak-date. Graphical output provided by the AeRobiology R package (Rojo et al., 2019). The average percentage of total pollen registered before the start-date of the pollen season in Toledo was 2.5%.

References

- Cornes, R.C., van der Schrier, G., van den Besselaar, E.J.M., Jones, P.D., 2018. An Ensemble Version of the E-OBS Temperature and Precipitation Data Sets. *J. Geophys. Res. Atmospheres* 123, 9391–9409. <https://doi.org/10.1029/2017JD028200>
- European Union, Copernicus Land Monitoring Service, 2020. Corine Land Cover. 2018, European Environment Agency (EEA) [WWW Document]. URL <https://land.copernicus.eu/> (accessed 1.12.20).
- Fick, S.E., Hijmans, R.J., 2017. WorldClim 2: new 1-km spatial resolution climate surfaces for global land areas. *Int. J. Climatol.* 37, 4302–4315. <https://doi.org/10.1002/joc.5086>
- Klein Tank, A.M.G., Wijngaard, J.B., Können, G.P., Böhm, R., Demarée, G., Gocheva, A., Mileta, M., Pashiardis, S., Hejkrlik, L., Kern-Hansen, C., Heino, R., Bessemoulin, P., Müller-Westermeier, G., Tzanakou, M., Szalai, S., Pálsdóttir, T., Fitzgerald, D., Rubin, S., Capaldo, M., Maugeri, M., Leitass, A., Bukantis, A., Aberfeld, R., van Engelen, A.F.V., Forland, E., Mietus, M., Coelho, F., Mares, C., Razuvaev, V., Nieplova, E., Cegnar, T., Antonio López, J., Dahlström, B., Moberg, A., Kirchhofer, W., Ceylan, A., Pachaliuk, O., Alexander, L.V., Petrovic, P., 2002. Daily dataset of 20th-century surface air temperature and precipitation series for the European Climate Assessment: EUROPEAN TEMPERATURE AND PRECIPITATION SERIES. *Int. J. Climatol.* 22, 1441–1453. <https://doi.org/10.1002/joc.773>
- Rivas-Martínez, S., Penas, Á., del Río, S., González, T.E.D., Rivas-Sáenz, S., 2017. Bioclimatology of the Iberian Peninsula and the Balearic Islands, in: The Vegetation of the Iberian Peninsula. Springer, pp. 29–80.
- Rivas-Martínez, S., Rivas-Saenz, S., Penas, A., 2011. Worldwide bioclimatic classification system. *Glob. Geobot.* 1, 1–634.
- Rojo, J., Picornell, A., Oteros, J., 2019. AeRobiology: the computational tool for biological data in the air. *Methods Ecol. Evol.* 2041–210X.13203. <https://doi.org/10.1111/2041-210X.13203>